doi:10.1006/jmbi.2001.4735 available online at http://www.idealibrary.com on IDEAL® *J. Mol. Biol.* (2001) **310**, 141–156

JMB

Vps9, Rabex-5 and DSS4: Proteins with Weak but Distinct Nucleotide-exchange Activities for Rab Proteins

Heike Esters[1], Kirill Alexandrov[1], Andrei Iakovenko[1], Tania Ivanova[1] Nicolas Thomä[1], Vladimir Rybin[2], Marino Zerial[2], Axel J. Scheidig[1] and Roger S. Goody[1]*

[1]*Department of Physical Biochemistry, Max-Planck Institute for Molecular Physiology, Otto-Hahn-Strasse 11, 44227 Dortmund Germany*

[2]*European Molecular Biology Laboratory, Meyerhofstrasse 69012 Heidelberg, Germany*

**Corresponding author*

The activities of three Rab-specific factors with GDP/GTP exchange activity, Vps9p, Rabex-5 and DSS4, with their cognate GTPases, Ypt51p, Rab5 and Ypt1p, have been analysed quantitatively. In contrast to other exchange factors examined and to DSS4, Vps9p, and by analogy probably Rabex-5, have considerably lower affinity than GDP to the respective GTPases. In keeping with this, they are relatively weak exchangers, with a maximal rate constant for GDP release from the ternary complex between exchange factor, GTPase and GDP of ca 0.01 s^{-1}, which is several orders of magnitude lower than for other exchange factors examined. If interaction with these proteins is a mandatory aspect of the Rab cycle, this suggests that the overall rate of cycling might be controlled at this point of the cycle. Surprisingly, DSS4, which has the thermodynamic potential to displace GDP effectively from Ypt1p, also does this very slowly, again with a maximal rate constant of ca 0.01 s^{-1}. An additional, and based on present knowledge, unique, feature of the Ypt1p.DSS4 complex, is that the association of GTP (or GDP) is more than 10^3-fold slower than to Ypt1p, thus leading to a long life-time of the binary complex between the two proteins, even at the high nucleotide concentrations that prevail in the cell. This leads to the conclusion that the protein-protein complex is likely to have an important biological significance in addition to its probable role in GTP/GDP exchange.

Keywords: Rab proteins; exchange factors; Vps9; Rabex-5; DSS4

Introduction

Rab proteins are ubiquitous regulators involved in vesicular transport in eukaryotic cells.[1–5] Although their functional mechanism is not yet fully understood, Rab/Ypt proteins are known to act as regulators of targeting and fusion of transport vesicles with their destined compartment and of motility of vesicles along cytoskeletal filaments.[6,7] They perform these functions by interacting with several distinct effector proteins. In common with other members of the Ras superfamily of small GTP-binding proteins (GTPases), they cycle between an inactive GDP-bound and an active GTP-bound state. The transition between these two states is governed by GTP hydrolysis and GDP dissociation (with subsequent GTP association), processes that are regulated by distinct activities of additional protein factors. These are the GAPs (GTPase-activating proteins) and GEFs (GDP/GTP-exchange factors), which, as for other members of the Ras superfamily, accelerate these intrinsically slow processes by several orders of magnitude. While quantitative data are available for the interaction of Rab proteins with their respective GAP molecules (at least in the case of the yeast Rab proteins termed Ypt[8,9]), only a lim-

Present address: T. Ivanova, Department of Anatomy and Cell Biology, University of Ulm, D-89069 Ulm, Germany.

Abbreviations used: GAPs, GTPase-activating proteins; GEFs, GDP/GTP-exchange factors; GppNHp, guanosine 5′-*O*-(β-γ-imidodiphosphate); ESI-MS, electrospray ionization mass-spectrometry; FRET, fluorescence resonance energy transfer.

E-mail address of the corresponding author: goody@mpi-dortmund.mpg.de

0022-2836/01/010141–16 $35.00/0

ited number of data are available for Rab-GEFs, although several proteins have been identified that show exchange activity. Known Rab-specific proteins showing exchange activity can be separated roughly into two categories based on their substrate specificity. On the one hand, proteins such as Sec2, Vps9, Rabex-5 and Rab3a GEF are active on a single cognate Rab GTPase.[10–13] On the other hand, proteins originally identified as exchange factors, Mss4 and DSS4, are active on a subset of Rab/Ypt proteins.[14–17] It has in fact been questioned whether the latter proteins function as genuine exchange factors.[18,19]

Here, we report the detailed kinetic characterisation of the interaction of Ypt51p with Vps9p,[20] of Rab5 with Rabex-5[12] and of Ypt1p with DSS4.[16]

Results

The results obtained are discussed in terms of the coupled equilibria shown in Scheme 1 (G is the GTPase, GXP is GDP or GTP and GEF the guanine nucleotide exchange factor).

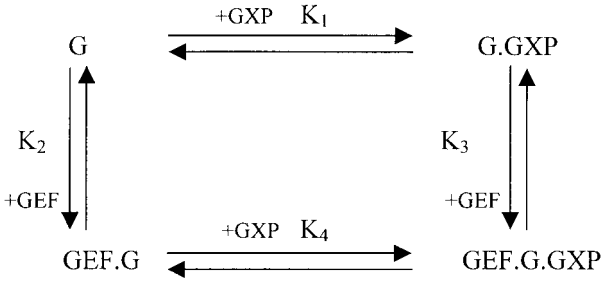

Scheme 1o

Simple thermodynamic considerations require that in scheme 1, $K_1 \times K_3 = K_2 \times K_4$ or in a more useful form:

$$\frac{K_1}{K_4} = \frac{K_2}{K_3} \qquad (1)$$

Equation (1) will be referred to throughout the work. Expressed verbally, it means that if the interaction of GEF with G weakens its affinity for GDP (or GTP), then the converse applies in the same measure (i.e. the interaction of GDP with G weakens its affinity for GEF). The basic mechanism of GEFs is based on this effect, although the principle can be modified further by differential effects on individual kinetic constants, as discussed below.

Interaction of Ypt1p and Ypt51p with guanosine nucleotides

Methods developed previously for examining the kinetics of GDP and GTP interaction with GTPases[21–23] were applied to the two Ypt proteins used here. The proteins contain conserved tryptophan residues (positions 62 and 102 in Ypt1p, 61 and 101 in Ypt51p), and the fluorescence signal from these residues is sensitive to the nucleotide at the active site. For both proteins, the fluorescence intensity was highest for the GDP-bound state and decreased significantly (ca 50 % for Ypt51p and somewhat less for Ypt1p) in the GTP-bound state. The nucleotide-free proteins showed intermediate fluorescence intensities. It is of interest to note that the same qualitative behaviour was observed for Rab5 and Rab7,[21] both of which also have tryptophan residues at equivalent positions. While it is not possible on the basis of present evidence to decide which of the trytophan residues contributes to the signal change seen, it is noteworthy that the residue at position 61 (or 62) immediately precedes the aspartate residue of the highly conserved WDTAGQE sequence. This aspartate residue is an indirect (*via* a water molecule) ligand of the magnesium ion associated with the nucleotide in the 3-D structure of Ypt51p.[24] The residues between alanine residue 64 (or 65) and the start of the next alpha helix (alanine residue 70 or arginine 71) constitute the catalytically important loop 4 region, or switch II, which is presumed to undergo major structural changes on GTP hydrolysis. Thus, we speculate that it is likely that the changes in the tryptophan signal reflect this transition.

These changes in tryptophan fluorescence could be used to monitor the time-course of the interactions in a time-dependent manner. The individual time-courses could be fitted as single exponentials as long as nucleotide was present in large excess over nucleotide-free protein. In all cases (i.e. Ypt1p or Ypt51p with GTP or with GDP), plots of the observed pseudo first-order rate constant against the nucleotide concentration were hyperbolic, as shown in Figure 1 for Ypt51p and GTP. This is similar to the behaviour seen with other GTPases[22,25] and is indicative of a two-step binding mechanism in which a rapid but weak equilibrium is followed by a relatively slow isomerisation, interpreted as a conformational change of the protein-nucleotide complex, as shown in Scheme 2:

$$\mathrm{Ypt51 + GXP} \underset{}{\overset{K_{1a}}{\rightleftarrows}} \mathrm{Ypt51.GXP} \underset{k_{-b}}{\overset{k_{+1b}}{\rightleftarrows}} \mathrm{Ypt51*.GXP}$$

Scheme 2.

Fitting a hyperbolic curve to the data of Figure 1 leads to values for K_{1a} and k_{+1b}.[22] Within the limits of error, the fitted curve passes through the origin of the graph. This shows that the value of k_{-1b} (which controls the overall rate of dissociation) is too small to be estimated by this method. The dissociation rate of the fluorescent GDP analog, mantGDP, could be measured directly by displacing it from its complex with Ypt1p or Ypt51p with a large excess of unlabelled GDP (data not

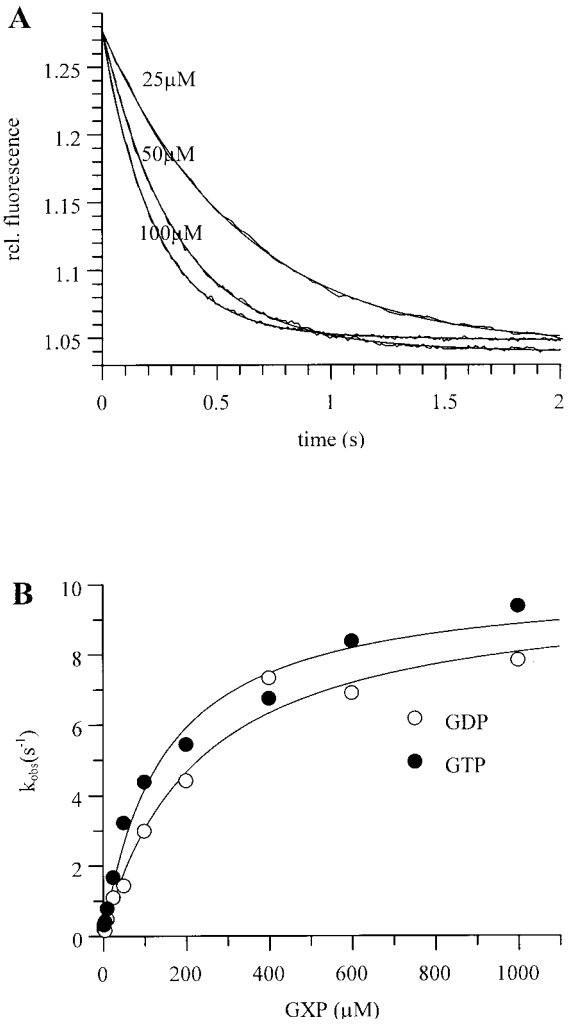

Figure 1. (a) Association kinetics of nucleotide-free Ypt51p (0.5 μM) and different concentrations of GTP. Formation of the complex was monitored by tryptophan fluorescence in a stopped-flow apparatus. Pseudo first-order rate constants were obtained from single-exponential fits to the data. (b) Dependence of the pseudo first-order rate constant of association of GDP/GTP with nucleotide-free Ypt51p on the concentration of the respective nucleotide.

shown). As described previously for Rab5 and Rab7,[21] advantage could be taken of the fact that energy transfer occurs between the protein tryptophan residues and the methylanthraniloyl group, resulting in a large signal change on interaction of the labelled nucleotide with the protein. It was assumed that the fluorescent label on the nucleotide does not have a major influence on the nucleotide dissociation rate constant, as already shown for other GTPases.[22,25]

The values obtained for the constants of Scheme 2 are given in Tables 1 and 2. The product of K_{1a} and k_{+1b} is referred to as k_{on}, since it represents the effective second-order rate constant of association at low nucleotide concentration or, in other words, the initial slope of the hyperbola as shown in Figure 1. For the methylanthraniloyl derivatives, high concentrations of nucleotide could not be used in the association reaction, due to the high background fluorescence, so that only the initial slope of the hyperbola (corresponding to $K_{1a} \times k_{+1b}$) could be determined. The value of k_{-1b} for mantGppNHp is used as an estimate for the constant for GTP. Since it is known from previous work on other GTPases that the modification to the triphosphate moiety tends to increase the dissociation rate, this should be regarded as an upper limit for GTP.

The data presented in the Tables confirm the similarities between the two Ypt proteins and other small GTPases with respect to their nucleotide-binding properties. In comparison with Rab5,[21] the overall affinity is a factor of ca 10 lower for Ypt1p and Ypt51p. This effect arises mainly from an increased dissociation rate (k_{-1b}) for Ypt1p, whereas for Ypt51p it arises from a combination of reduced association and increased dissociation rate constants. Rab7 displays even tighter binding (a factor of ca 100 higher than Ypt1p or Ypt51p), mainly due to a much faster effective association rate constant (3×10^6-5×10^6 M^{-1} s^{-1}).[21]

Kinetic characterisation of the Vps9p-Ypt51p-system: interaction of nucleotide-free Ypt51p and Vps9p

The association of Ypt51p and Vps9p resulted in a small increase in tryptophan fluorescence. Although this could not be used conveniently for equilibrium titration experiments, since both proteins contain tryptophan, the signal was perfectly adequate for stopped-flow experiments. This allowed the determination of the pseudo first-order rate constant for the association reaction as a function of the Vps9p concentration at constant Ypt51p concentration, as shown in Figure 2. It can be seen that there is a linear dependence of this rate con-

Table 1. Kinetic constants for the interaction between Ypt1p and guanosine nucleotides

	K_{1a} (M^{-1})	k_{+1b} (s^{-1})	k_{on} (M^{-1} s^{-1})	k_{-1b} (s^{-1})	K_1 (M^{-1})	$1/K_1$ (nM)
GDP	3.8×10^3	39.5	1.5×10^5	6×10^{-5}	2.5×10^9	0.40
mantGDP			1.7×10^5	6×10^{-5}	2.8×10^9	0.35
GTP	3.3×10^3	38.6	1.3×10^5	5×10^{-5}	2.5×10^9	0.39
MantGppNHp			1.4×10^5	5×10^{-5}	2.8×10^9	0.36

Table 2. Kinetic constants for the interaction between Ypt51p and guanosine nucleotides

	K_{1a} (M^{-1})	k_{+1b} (s^{-1})	k_{on} (M^{-1} s^{-1})	k_{-1b} (s^{-1})	K_1 (M^{-1})	$1/K_1$ (nM)
GDP	4.5×10^3	9.9	4.5×10^4	2×10^{-5}	2.2×10^9	0.45
mantGDP			7.3×10^4	2×10^{-5}	3.7×10^9	0.27
GTP	7.1×10^3	10.1	7.2×10^4	3×10^{-5}	2.4×10^9	0.42
mantGppNHp			5.8×10^4	3×10^{-5}	1.9×10^9	0.52

stant on the Vps9p concentration and that, within the limits of experimental error, the linear fit passes through the origin, suggesting a very low rate for the dissociation reaction. The association rate constant, which is given by the slope of the straight line in the Figure, has a value of 3.1×10^5 M^{-1} s^{-1}. We refer to this constant as k_{+2}, since the interaction corresponds to that described by K_2 in Scheme 1.

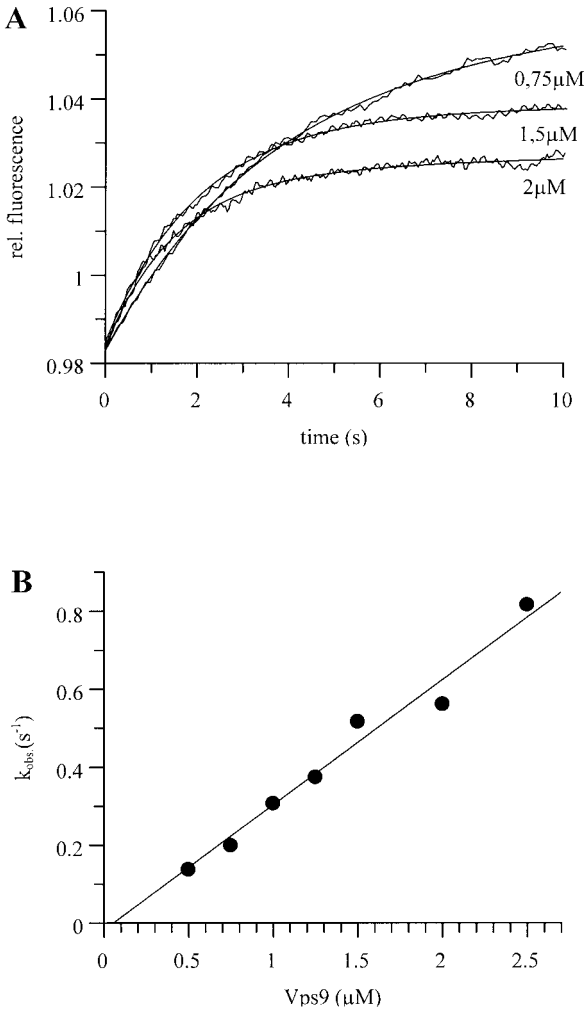

Figure 2. (a) Association kinetics of nucleotide-free Ypt51p (0.25 μM) and different concentrations of Vps9p. Data were collected using a stopped-flow apparatus with tryptophan fluorescence as a signal of binding. Individual curves were fitted with single-exponential terms. (b) Dependence of the pseudo first-order rate constant for the association of nucleotide-free Ypt51p on the concentration of Vps9p.

In order to measure k_{-2}, one of the two protein components of the system must be available in a form that is spectroscopically distinguishable from the essentially wild-type proteins used so far. In an initial attempt to achieve this, a mutant of Ypt51p that contained no tryptophan residues, Ypt51p(W61FW101F), was prepared. However, this mutant was not stable enough in the nucleotide-free form to allow it to be used to displace the wild-type protein from its complex with Vps9p. We therefore adopted the strategy of labelling Vps9p with a fluorescent group for this purpose. Labelling with dansyl chloride led to introduction of two dansyl groups, as shown by electrospray ionization mass spectrometry (ESI-MS) (spectra not shown). Association of dansyl-labelled Vps9p with nucleotide-free Ypt51p leads to an increase in fluorescence of the label. As shown in Figure 3, this signal could be used to monitor the kinetics of the association reaction. The dependence of the pseudo first-order rate constant on the Ypt51p concentration was linear and corresponded to an association rate constant of $k_{+2} = 2.9 \times 10^5 M^{-1}s^{-1}$, in good agreement with the value obtained with unlabelled proteins ($k_{+2} = 3.1 \times 10^5 M^{-1}s^{-1}$).

The dissociation rate constant of labelled Vps9p from its complex with Ypt51p was determined by displacement with unlabelled Vps9p (data not shown). The single exponential fit to the curve obtained gave a rate constant of $k_{-2} = 4.7 \times 10^{-3}$ s^{-1}. Taking the ratio of the reverse and forward constants to give the K_d for the interaction leads to a value of 15.2 nM. This corresponds to $1/K_2$ in Scheme 1.

Interaction of the Vps9p.Ypt51p complex with guanosine nucleotides

On interaction of the complex between the two proteins with GTP or GDP, there was a decrease in tryptophan intensity. The pseudo first-order rate constant determined from such curves as those shown in Figure 4(a) increased hyperbolically with increasing GTP concentration (Figure 4(b)). This behaviour is interpreted in terms of a two-step mechanism, in which a weak initial binding is followed by a second step, which is either the dissociation of the protein-protein complex or a rate-limiting isomerisation that precedes this. To distinguish between these two possibilities, we repeated this experiment with a large excess of

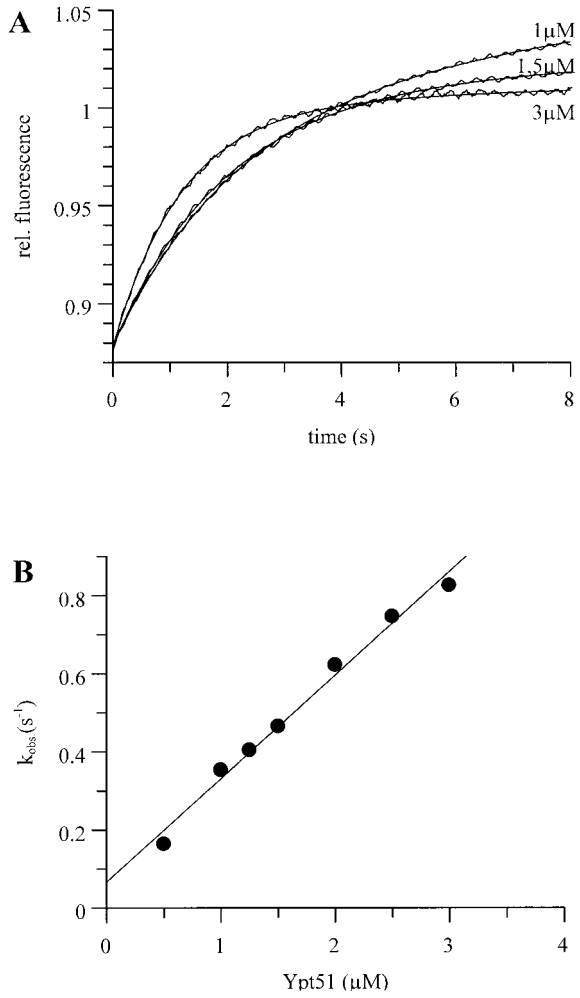

Figure 3. (a) Time-course of the FRET signal change seen in mixing 0.25 μM dansyl-labelled Vps9p with different concentrations of nucleotide-free Ypt51p in the stopped-flow apparatus. The fits shown are to a single-exponential equation. (b) Dependence of the observed rate constants for the association reaction on the concentration of nucleotide-free Ypt51p.

Vps9 over Ypt51p. Under these conditions the observed association rates were essentially identical with those obtained in the experiment described above, thus indicating that the fluorescence change comes from nucleotide interaction with Vps9p.Ypt51p complex and not with nucleotide-free Ypt51p (data not shown). The values of the constants for these two processes are $K_{4a} = 2.3 \times 10^3 M^{-1}$ and $k_{+4b} = 24.3\ s^{-1}$ for GTP, and $K_{4a} = 1.5 \times 10^4\ M^{-1}$ and $k_{+4b} = 20.8\ s^{-1}$ for GDP, respectively (constants named according to the two-step binding mechanism of Scheme 2).

Similar experiments could be performed using dansyl-labelled Vps9p. The rate of the decrease in dansyl fluorescence observed on interaction of GTP or GDP with the complex between Ypt51p and labelled Vps9p showed a concentration-dependence similar to that seen using intrinsic tryptophan fluorescence (data not shown; results summarized in Table 3). Finally, this process could be observed using fluorescently labelled nucleotides with unlabelled proteins. Only a limited concentration range of these nucleotides could be used, due to the high background fluorescence caused by excess nucleotide, but their behaviour was quantitatively similar to that of unlabelled nucleotides. These data suggest that the method chosen for labelling nucleotides and Vps9p did not have a major effect on their interactions with Ypt51p. The results are summarized in Table 3.

Interaction of Vps9p with Ypt51p-nucleotide complexes

Addition of Vps9p to a complex between Ypt51p and mantGDP led to relatively slow release of a small fraction of the bound nucleotide. As can be seen in Figure 5(a), at 150 nM Ypt51p.mantGDP, 3 μM Vps9p led to ca 10% release of bound nucleotide. This is understandable in qualitative terms, since there is a strong competitive component in binding of nucleotide and exchanger in such systems, and the data presented above show that mantGDP is bound ca 60-fold more strongly than Vps9p, so that high concentrations of Vps9p are needed to compete with nucleotide binding in this equilibrium situation. Complete displacement of the fluorescent nucleotide was observed on addition of excess unlabelled GDP. As shown in Figure 5(b), there was a hyperbolic dependence of the rate constant for mantGDP release on the Vps9p concentration, which saturated at an extrapolated value of $1.2 \times 10^{-2}\ s^{-1}$ with an apparent K_d value of 2.3×10^{-5} M. These values

Table 3. Kinetic constants for nucleotide association with the Vps9p.Ypt51p complex. The asterisk denotes measurements obtained using dansyl-labelled Vps9p

	K_{4a} (M^{-1})	$1/K_{4a}$ (μM)	k_{+4b} (s^{-1})	k_{on} ($M^{-1}\ s^{-1}$)
GDP	1.5×10^4	64.9	20.8	3.2×10^5
mantGDP				2.1×10^5
GDP*	1.3×10^4	78	22.5	2.9×10^5
GTP	2.3×10^3	436.5	24.3	5.6×10^4
MantGppNHp				3.2×10^4
GTP*	2.5×10^3	403	23.2	5.8×10^4

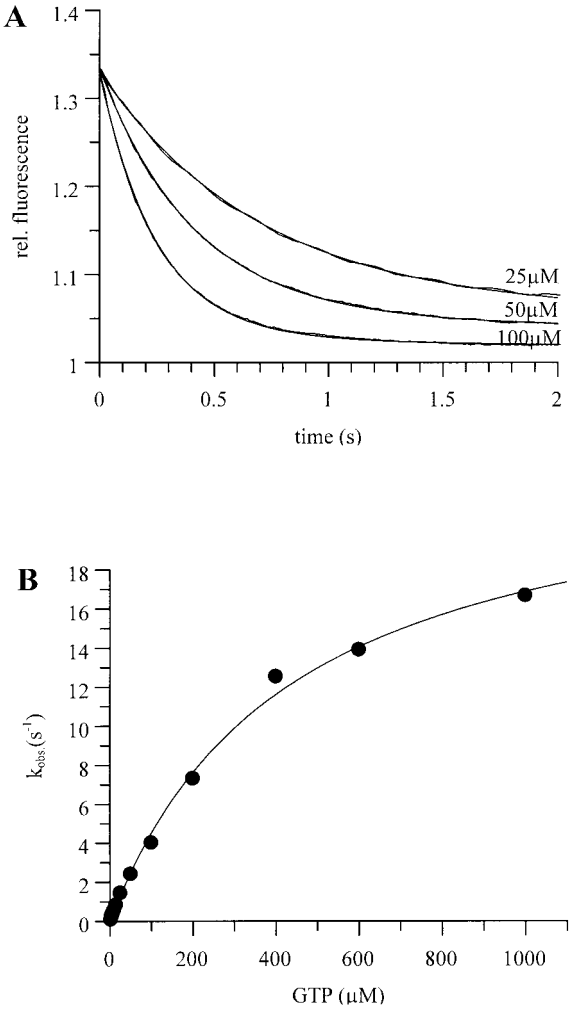

Figure 4. (a) Interaction of Vps9p.Ypt51p (0.5 μM) complex and different concentrations of GTP. The Tryptophan signal used in the stopped-flow apparatus to monitor the reaction decreased. (b) Dependence of the observed rate constants for the association reaction on the concentration of GTP.

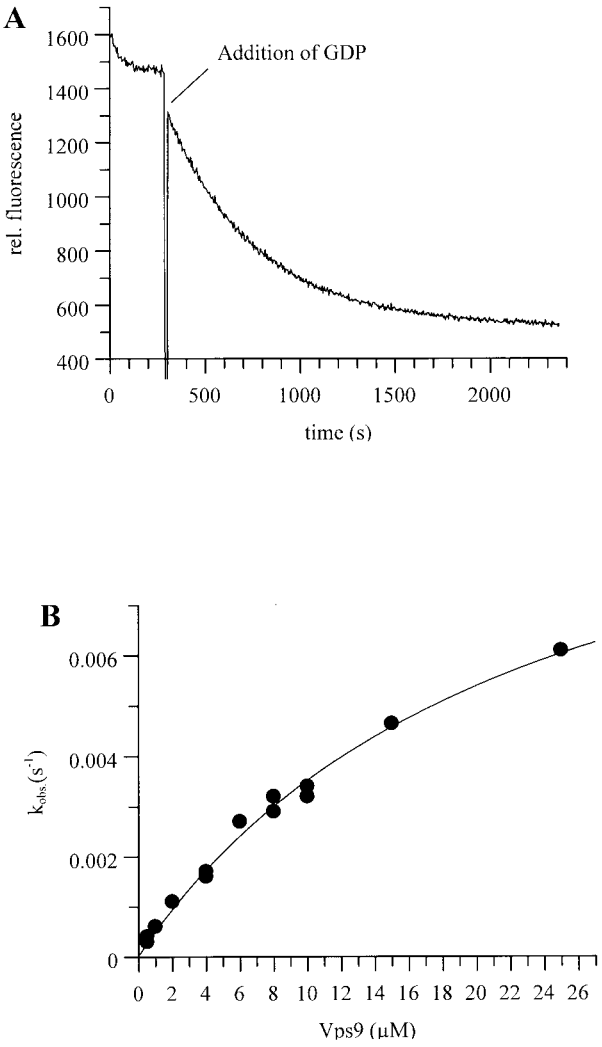

Figure 5. (a) Interaction of Vps9p with Ypt51p.-mantGDP (150 nM). The data were collected with an SLM 8100 spectrophotometer *via* the FRET signal. In the first part of the curve, the fluorescence change after adding 3 μM Vps9p is shown. In the second part of the curve, the rate constant for mantGDP release could be measured after addition of excess unlabelled GDP (50 μM). (b) Dependence of the rate constant for mantGDP release on the Vps9p concentration.

correspond to the constants $1/K_3$ and k_{-4} respectively, in Scheme 1.

It is of interest to note that the first phase in Figure 5(a), which arises from displacement of mantGDP under the influence of Vps9p alone (i.e. without an unlabelled displacing nucleotide), did not increase significantly in amplitude at high Vps9p concentrations. Although the quality of the data obtained was not adequate for a quantitative analysis (due to the relatively small signal amplitude and low stability at long measurement times), this is already an indication that the affinity of mantGDP in the ternary complex with Ypt51p and Vps9p is still relatively high, since complete dissociation cannot be induced by Vps9p even at the low prevailing total protein bound nucleotide concentration of 150 nM. Since the data suggest that less than 50 % of the mantGDP can be displaced, a simple calculation shows that its K_d value (corresponding to $1/K_4$) must be less than 75 nM. This corresponds well with the value of 37 nM, which can be calculated from analysis of the complete scheme as described below.

The influence of Vps9p on the dissociation of mantGppNHp from its complex could not be examined quantitatively. On increasing the Vps9p concentration in the range of 0.5 to 10 μM, an approximately tenfold increase in the nucleotide dissociation rate (from 3×10^{-5} s^{-1} (k_{-1b}) in the absence of the exchange factor to 3.8×10^{-4} s^{-1}

(k_{-4b}) in its presence) was observed, but accurate estimation of the extremely slow process was difficult due to problems of stability and photobleaching.

These results can be interpreted in two principally different manners. In one model, GTP and Vps9p binding to Ypt51p are highly competitive, so that the ternary complex is very unstable, and other GTPases, it seems reasonable to expect an analogous process to occur when GDP or GTP bind to the Vps9p.Ypt51p complex. We have thus considered two alternative models (A and B) for the association of GDP with the binary protein complex and assigned rate and equilibrium constants arising from the experiments described using the nomenclature of Scheme 1. Model B

Model A

$$\text{Vps9.Ypt51} + \text{GDP} \underset{k_{-4}}{\overset{k_{+4}}{\rightleftarrows}} \text{Vps9.Ypt51.GDP} \underset{k_{+3}}{\overset{k_{-3}}{\rightleftarrows}} \text{Ypt51} * \text{.GXP} + \text{Vps9}$$

$$K_4 = \frac{k_{+4}}{k_{-4}} \qquad K_3 \frac{k_{+3}}{k_3}$$

Model B

$$\text{Vps9.Ypt51} + \text{GDP} \overset{K_{4a}}{\rightleftarrows} \text{Vps9.Ypt51.GDP} \underset{k_{-4b}}{\overset{k_{+4b}}{\rightleftarrows}} \text{Vps9.Ypt51} * \text{GDP} \underset{k_{+3}}{\overset{k_{-3}}{\rightleftarrows}} \text{Ypt51} * \text{GDP} + \text{Vps9}$$

$$K_4 = \frac{K_{4a} \times k_{+4b}}{k_{4b}} \qquad K_3 = \frac{k_{+3}}{k_{-3}}$$

Scheme 3.

significant generation of this complex, which would be a prerequisite for acceleration of GTP dissociation, could occur only at very high Vps9p concentrations. In the second possibility, which would seem unlikely for a protein whose properties are those of an exchange factor, Vps9p and Ypt51p.GTP would form a relatively stable complex from which both GTP and Vps9p can dissociate only slowly. To distinguish between these possibilities, the Ypt51p.GppNHp complex was tested as an inhibitor of the influence of Vps9p on the dissociation of mantGDP from its complex with Ypt51p. In a series of experiments (data not shown), the influence of Ypt51p.GppNHp on the exchange kinetics of 150 nM Ypt51p.mantGDP in the presence of 5 μM Vps9p and 50 μM GDP were examined. No influence was detected, even when Ypt51p.GppNHp was present in twofold excess (10 μM) over Vps9p. This suggests that the affinity of Vps9p for the GTP-form of Ypt51p is weak (1/K_3 value of greater than 10 μM).

Analysis of the data from the three-component system consisting of Vps9p, Ypt51p and GDP

A fundamental question to be answered in analysing the data obtained is concerned with whether the ternary complex between the proteins and the nucleotide can exist in more than one form. Since it is clear from the data on interaction of nucleotides with Ypt51p that there is a two-step binding mechanism involving a protein isomerisation, as with includes an additional isomerisation step of the ternary complex.

In model A, K_4 is 1.5×10^4 M^{-1} and k_{-3} is 20.8 s^{-1}. K_4 in model A corresponds to K_{4a} in model B and k_{-3} in model A corresponds to k_{+4b} in model B. k_{-4} in model A corresponds to k_{-4b} in model B and has the value of $1.2 \times 10^{-2} s^{-1}$. For model B, we can define K_4 in the sense of Scheme 1 as being equal to $K_{4a} \times k_{+4b}/k_{-b}$ and it has the value of $2.7 \times 10^7 M^{-1}$. Thus, in terms of Scheme 1, the only quantitative difference between the two models is in the value of K_4, which is 1.5×10^4 M^{-1} for model A and 2.7×10^7 M^{-1} for model B. Since the relationship $K_1 \times K_3 = K_2 \times K_4$ must hold for both models, this can be used to test their consistency. In model A, $K_1 \times K_3$ has the value 9.5×10^{13} M^{-2}, while $K_2 \times K_4$ has the value 9.9×10^{11} M^{-2}. Thus, there is a discrepancy of a factor of 100. In model B, $K_1 \times K_3$ is again 9.5×10^{13} M^{-2}, and $K_2 \times K_4$ is 1.8×10^{15} M^{-2}. Thus in this case, the discrepancy is considerably smaller (a factor of ca 20). Although this is still quite large, it must be remembered that the individual rate constants in the Scheme were determined using different signals, i.e. some measurements were with unlabelled proteins and unlabelled nucleotides, whereas others used labelled proteins or labelled nucleotides, so that accumulation of small errors could lead to the relatively large discrepancy.

The better quantitative agreement of model B than model A leads to the conclusion that it is reasonable to use model B as the minimum

mechanism for the interaction of GDP with Vps9.Ypt51p. This can be incorporated into Scheme 1 to lead to the following extended diagram which summarizes the data and interpretations discussed so far:

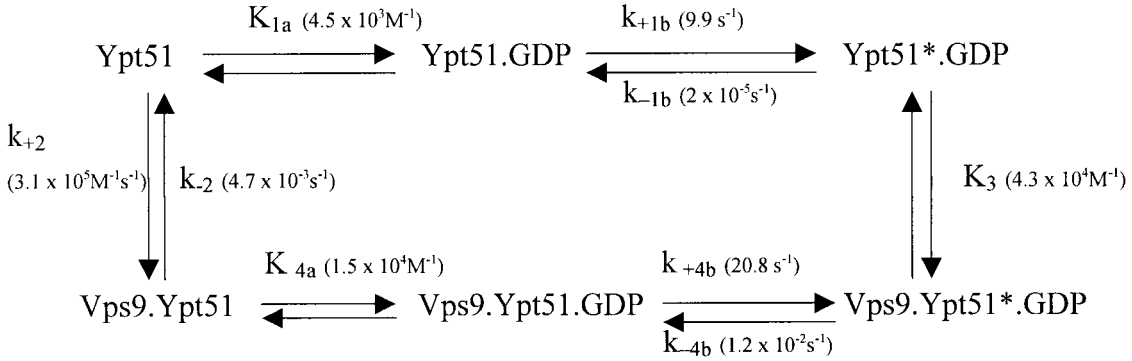

Scheme 4.

An attractive feature of this Scheme is that the isomerisation occurring on interaction of GDP with nucleotide-freeYpt is reflected by a similar process when GDP binds to the Vps9p.Ypt51p complex. The equilibrium constants for the first step (K_{1a} and K_{4a}, respectively) have similar values, as does the forward rate constant for the isomerisation step (k_{+1b} and k_{+4b}). The isomerisation step of the ternary complex can be regarded as involving a transition between two forms of Ypt51p, one of which binds nucleotide weakly (Ypt51p.GDP) but Vps9p strongly, while the other (Ypt51p*.GDP) binds nucleotide strongly but Vps9p weakly.

The constants for the interaction of Ypt51p, Vps9p and nucleotides are summarized in Table 4.

Exchange activity of Rabex-5

The mammalian protein that is analogous to Vps9p is Rabex-5, and its cognate GTPase is Rab5. In order to compare its properties with those of Vps9p, we carried out extensive experiments aimed at expressing adequate amounts of the protein. However, this was only partially successful, and the best strategy identified led only to small amounts of soluble protein. An extensive series of experiments on the interaction with Rab5 were precluded by the small quantities available and by the very low stability of Rabex-5. Due to these limitations, only one type of experiment was performed, which was the catalysis of nucleotide dissociation from Rab5. As shown in Figure 6(a), individual experiments were qualitatively similar to those with Vps9p, i.e. addition of Rabex-5 to Rab5.mantGDP led to a small extent of nucleotide release but, on addition of excess unlabelled GDP, complete dissociation of mantGDP could be achieved at a rate that was dependent on the Rabex-5 concentration (Figure 6(b)). The concentration dependence of the rate constant showed saturation behaviour with a maximum of 7.4×10^{-3} s^{-1}, of the same order of magnitude as that observed for Vps9p and Ypt51p (1.2×10^{-2} s^{-1}). However, the concentration dependence was quantitatively different, with an apparent K_d between Rabex-5 and Rab5.mantGDP of 270 nM, compared with 23 μM for Vps9p and Ypt51p.-mantGDP (see Figure 5). Assuming that the same basic mechanism pertains for this system as for Vps9p.Ypt51p, the value of $7.4 \times 10^{-3}s^{-1}$ corresponds to k_{-4b} and 270 nM to $1/K_3$ in Scheme 4. As in the Vps9p.Ypt51p system, displacement of the GTP analog mantGppNHp from its complex

Table 4. Summary of kinetic and thermodynamic constants for the interaction of the Ypt51p, Vps9p and guanosine nucleotides

GDP:			
$K_{1a} = 4.5 \times 10^3$ M^{-1}	$k_{+2} = 3.1 \times 10^5$ $M^{-1}s^{-1}$	$K_3 = 4.3 \times 10^4$ M^{-1}	$K_{4a} = 1.5 \times 10^4$ M^{-1}
$k_{+1b} = 9.9$ s^{-1}	$k_{-2} = 4.7 \times 10^{-3}$ s^{-1}		$k_{+4b} = 20.8$ s^{-1}
$k_{-1b} = 2 \times 10^{-5}$ s^{-1}	$K_2 = 6.6 \times 10^7$ M^{-1}		$k_{-4b} = 1.2 \times 10^{-2}$ s^{-1}
$K_1 = 2.2 \times 10^9$ M^{-1}			$K_4 = 2.7 \times 10^7$ M^{-1}
GTP:			
$K_{1a} = 7.1 \times 10^3$ M^{-1}	$k_{+2} = 3.1 \times 10^5$ M^{-1} s^{-1}	K_3= n.d.	$K_{4a} = 2.3 \times 10^3$ M^{-1}
$k_{+1b} = 10.1$ s^{-1}	$k_{-2} = 4.7 \times 10^{-3}$ s^{-1}		$k_{+4b} = 24.3$ s^{-1}
$k_{-1b} = 3 \times 10^{-5}$ s^{-1}	$K_2 = 6.6 \times 10^7$ M^{-1}		k_{-4b} = n.d.
$K_1 = 2.4 \times 10^9$ M^{-1}			K_4 = n.d.

n.d., not determined.

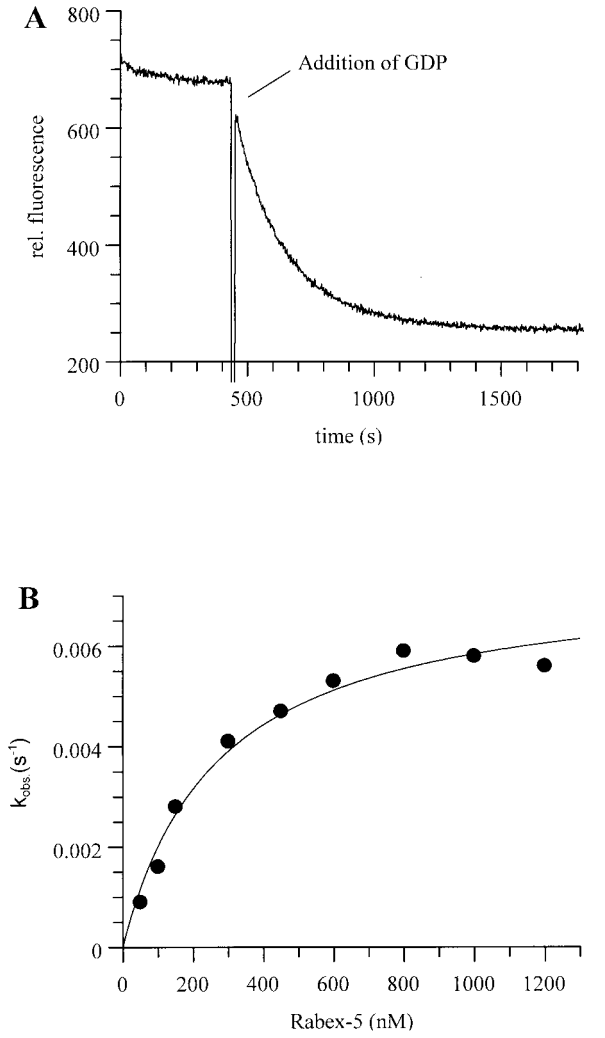

Figure 6. (a) Interaction of Rabex-5 and Rab5.-mantGDP. Data were collected using an SLM 8100 spectrophotometer with the FRET signal as a signal of the exchange reaction: 150 nM Rab5 and 600 nM Rabex-5 were mixed and in the second part of the curve, GDP was added to a final concentration of 50 μM. (b) Dependence of the observed rate constant for mantGDP release on the Rabex-5 concentration. The rate constants K_3 and k_{-4} could be determined from the fitted hyperbolic curve.

with Rab5 by Rabex-5 was much less efficient than for mantGDP. At 25 °C, the reaction was so slow that it could not be measured conveniently. At 37 °C, data were obtained (not shown) that showed a linear dependence of the observed first order rate constant on the Rabex-5 concentration. The slope of the fitted line was ca 10^3 $M^{-1}s^{-1}$, corresponding to $K_3 \times k_{-4b}$ in Scheme 4 and can be compared with the value of 7.25×10^4 $M^{-1}s^{-1}$ that can be calculated for mantGDP under these conditions (at 37 °C, k_{-4b} was $1.8 \times 10^{-2}s^{-1}$ and $1/K_3$ was 248 nM for mantGDP).

Thus, at low concentrations of Rabex-5, GDP appears to be displaced almost two orders of magnitude more effectively than GTP (taking GppNHp as a model substance) by Rabex-5.

Kinetic characterization of the DSS4-Ypt1p-system: interaction of nucleotide-free Ypt1p and DSS4

The interaction of nucleotide-free Ypt1p and DSS4 could be monitored by tryptophan fluorescence, since there was a reduction of intrinsic fluorescence on interaction of the two proteins. The dependence of the pseudo first-order rate constant for the association reaction on the concentration of DSS4 shows a linear dependence (data not shown), from which the association rate constant (k_{+2}) can be calculated to be 1.02×10^6 M^{-1} s^{-1}.

In order to measure the dissociation rate constant of the DSS4.Ypt1p complex, a further signal was needed. By analogy to Vps9p, an attempt was made to label DSS4 with dansyl chloride. Although this led to fluorescently labelled protein, this was so unstable that it could not be used for kinetic experiments. In contrast, Ypt1p could be labelled with dansyl chloride to give a stable fluorescent protein. To check that the properties of the labelled protein were not significantly different from those of unlabelled protein, the association with DSS4 was examined. This led to an increase in fluorescence if the FRET signal was used and measuring the dependence of the rate constant for this change on the DSS4 concentration led to a rate constant (k_{+2}) of 1.4×10^6 M^{-1} s^{-1} for the association rate constant, in good agreement with the value of 1.02×10^6 M^{-1} s^{-1} from the intrinsic fluorescence signal. Thus, labelling the protein does not appear to have a major effect on the interaction of the two proteins.

The rate constant for dissociation (k_{-2}) of dansyl-labelled, nucleotide-free Ypt1p from its complex with DSS4 was measured by displacement with unlabelled nucleotide-free Ypt1p and was found to be 7.2×10^{-4} s^{-1}. The K_d ($1/K_2$ in Scheme 1) value for the interaction was calculated to be 0.7 nM ($K_2 = 1.42 \times 10^9$ M^{-1}). Thus, the affinity of nucleotide-free Ypt1p to DSS4 is ca 20 fold higher than that between nucleotide-free Ypt1p and GDP or GTP ($K_1 = 2.5 \times 10^9$ M^{-1} for both nucleotides).

Interaction of the DSS4.Ypt1p complex with guanosine nucleotides

Two useful signals were identified for monitoring the interaction of nucleotides with the DSS4.Ypt1p complex. One of these was the FRET signal resulting from binding of mantGDP or mantGppNHp. This reaction was surprisingly slow, as shown in Figure 7. The slope of the plot of k_{obs} against the nucleotide concentration was 1.5×10^2 $M^{-1}s^{-1}$ for mantGDP and 0.8×10^2 $M^{-1}s^{-1}$ for mantGppNHp, or a factor of ca 10^3 lower than for nucleotide association with

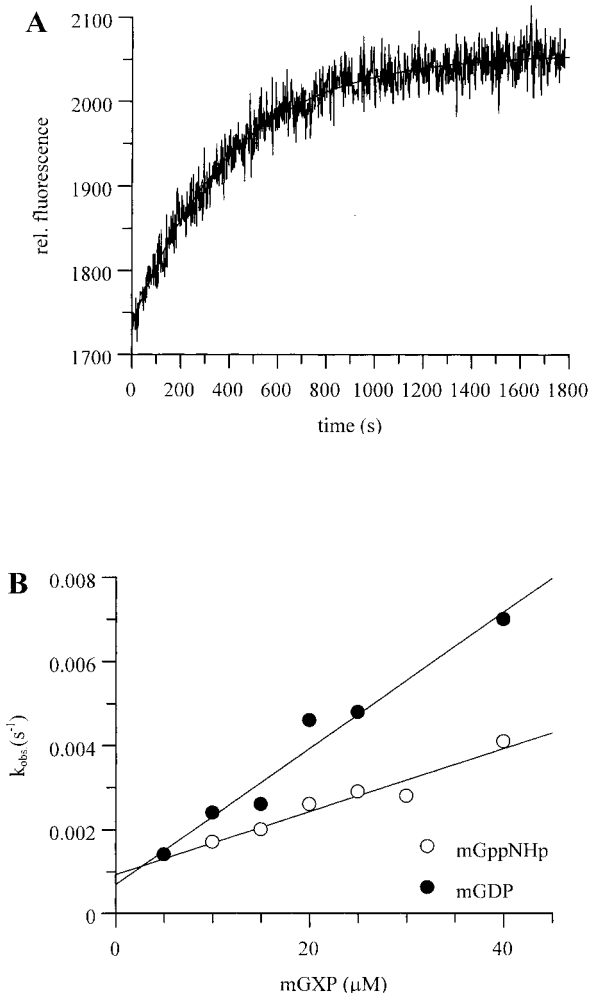

Figure 7. (a) Association reaction of mantGDP (10 μM) and 0.2 μM Ypt1p.DSS4 monitored using FRET. (b) Dependence of the observed rate constant for the association reaction on the mantGDP or mantGppNHp concentration.

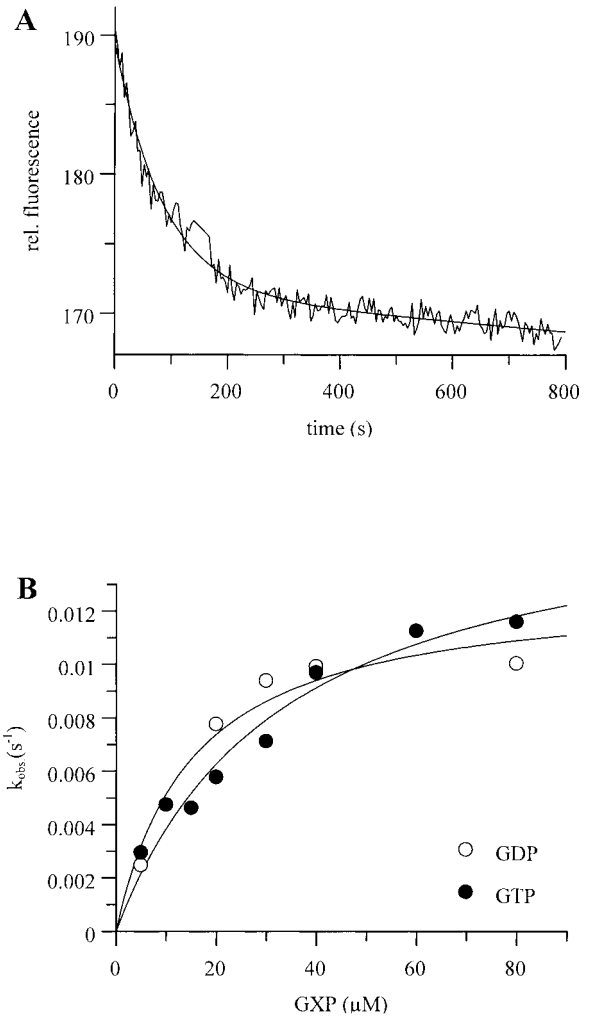

Figure 8. (a) Interaction of GDP/GTP with the complex of dansyl-labelled DSS4 and Ypt1p monitored by FRET. The association of 80μM GTP with 100 nM complex is shown. (b) Hyperbolic dependence of the pseudo first-order rate constant for the association of GDP or GTP.

the Vps9p.Ypt51p complex (mantGDP $k_{on} = 2.1 \times 10^5$ $M^{-1}s^{-1}$; mantGppNHp $k_{on} = 3.2 \times 10^4$ $M^{-1}s^{-1}$). Using the other signal identified for this interaction, i.e. the FRET signal observed using dansyl-labelled Ypt1, similar results were obtained, with the initial slope of the plot of the observed rate constant against the nucleotide concentration suggesting a second-order rate constant of ca 10^2 M^{-1} s^{-1} for GDP and GTP. In this case, considerably higher concentrations of nucleotides could be used, and it was clear that there was a hyperbolic dependence of the rate constant on the nucleotide concentration (Figure 8). The K_d values (corresponding to $1/K_4$ in scheme 1) were 15.1 μM and 31.1 μM, respectively, for GDP and GTP, while the maximal rate constants (interpreted as k_{-3}) were 1.3×10^{-2} s^{-1} for GDP and 1.6×10^{-2} s^{-1} for GTP. As shown in Table 5, the calculated k_{on} rates for nucleotides at low concentrations ($K_4 \times k_{-3}$) were somewhat higher for the natural nucleotides than for fluorescently labelled nucleotides. Although this rate is very slow, it is still more then tenfold faster than the spontaneous rate of dissociation of the DSS4.Ypt1 complex, excluding the possibility that GDP or GTP cannot associate until the binary complex has dissociated.

Interaction of DSS4 with Ypt1-nucleotide complexes

In contrast to the situation with Vps9p and Rabex-5, DSS4 was found to be thermodynamically highly effective in displacing nucleotides from their complexes with Ypt1 (Figure 9(a)). Under the conditions used (150 nM Ypt1.mantGDP), com-

Table 5. Kinetic constants for nucleotide association with the DSS4.Ypt1p complex

	K_4 (M^{-1})	$1/K_4$ (μM)	k_{-3} (s^{-1})	k_{on} (M^{-1} s^{-1})
GDP	6.6×10^4	15.1	1.3×10^{-2}	-
mantGDP	-	-	-	1.5×10^2
GTP	3.2×10^4	31.1	1.6×10^{-2}	-
MantGppNHp	-	-	-	0.8×10^2

plete displacement of mantGDP was observed using micromolar concentrations of DSS4. This was monitored in each experiment by the addition of unlabelled GDP, which would lead to the release of any remaining bound mantGDP or mantGppNHp.

Despite the effective displacement of protein-bound nucleotide, the rate of release was still very slow in comparison with the exchange factors for other members of the Ras-superfamily. Thus, the maximum rate constant for release of mantGDP from its DSS4.Ypt1.mantGDP complex (k_{obs} extrapolated from the data of Figure 9(b)) was 1.1×10^{-2} s^{-1}, compared to ca 20 s^{-1} for Ran and RCC1.[26] The corresponding constant for mantGppNHp, which could also be displaced effectively by DSS4, was 3.2×10^{-2} s^{-1}. The concentration-dependence of the observed rate constant for release of the mant nucleotides leads to an estimate of the K_d ($= 1/K_3$) value between DSS4 and the corresponding nucleotide-bound Ypt1. These are calculated to be 16.7 for mantGDP and 32.2 μM for mantGppNHp, respectively.

To test the validity of the assignment of rate and equilibrium constants, the same procedure as that used for Ypt51p and Vps9p was used. In this case, for GDP, $K_1 \times K_3$ has the value 1.5×10^{14} M^{-2}, while $K_2 \times K_4$ has the value 1.1×10^{14} M^{-2}. For GTP, $K_1 \times K_3$ is 5.4×10^{13} M^{-2}, and $K_2 \times K_4$ is 9.9×10^{13} M^{-2}. Thus there is good agreement, suggesting that the assignment of rate and equilibrium constants is correct. However, this does not mean that additional steps in the mechanism do not occur, but simply that the composite constants derived are a good quantitative reflection of the individual constants. Since the process described by K_1 is a two-step process, it seems likely that that described by K_4, i.e. the binding of nucleotide to the binary DSS4.Ypt1 complex, is also likely to involve two-steps. If we assume this to be the case, we can use a scheme identical with that used for Ypt51p and Vps9p, and the reason for the good quantitative agreement when comparing $K_1 \times K_3$ and $K_2 \times K_4$ becomes apparent. This is because in the additional step (described by k_{+4b} and k_{-4b}) the forward and reverse rate constants are essentially equal, giving an equilibrium constant of 1. Thus, the essential difference between the schemes for Ypt51p and Vps9p on the one hand and Ypt1 and DSS4 on the other is in this step, which has an equilibrium constant of ca 2000 in the former and of ca 1 in the latter case. This difference is completely due to the difference in k_{+4b}, and is compensated for by the much larger value of K_2 for this system than those for the Ypt51 and Vps9p systems (see Tables 4 and 6):

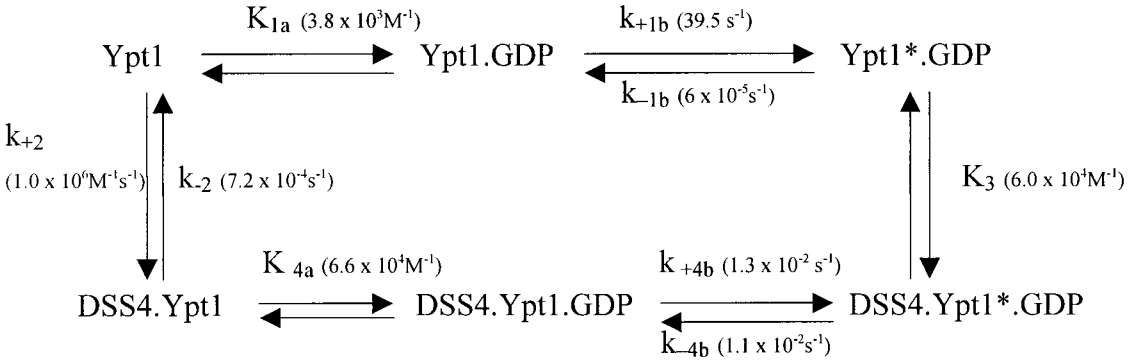

Scheme 5.

The constants for the interaction of GTP, Ypt1p and DSS4 show no major differences from those for GDP. They are summarized in Table 6.

Conclusions

The results described here represent a quantitative description of the activity of the three proteins Vps9p, Rabex-5 and DSS4 with their cognate Rab proteins, Ypt51p, Rab5 and Ypt1p. A feature they have in common is that in comparison to the well-characterized RCC1 (exchange factor for Ran[27–31]) and EF-Ts, exchange factor for EF-Tu,[32] they show relatively weak exchange activity, with a maximal rate constant for the release of GDP from its tern-

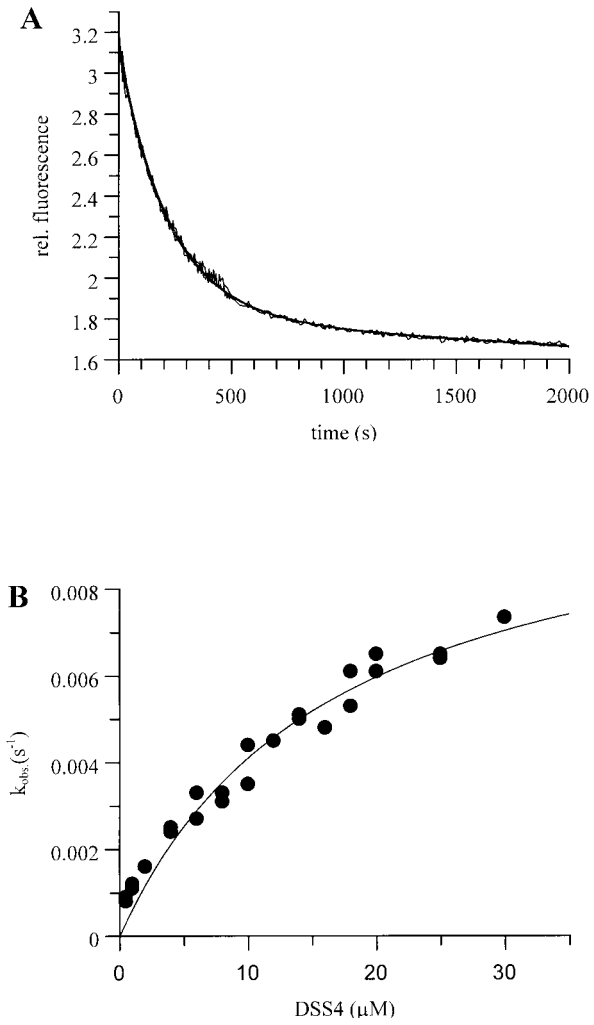

Figure 9. (a) DSS4-catalysed displacement of mantGDP from its complex with Ypt1p. Data shown monitor the reaction of 150 nM Ypt1p.mantGDP and 12 μM DSS4. Duplicate curves were measured using the Fluoroskan Ascent FL 1.8 fluorimeter *via* the FRET signal. (b) Plot of the determined rate constants against the DSS4 concentration gave a hyperbolic curve, leading to the constants K_3 and k_{-4}.

ary complex of ca 10^{-2} s^{-1} in all three cases. While this is very slow in comparison with Ran-RCC1 (ca 20 s^{-1}) and EF-Tu (ca 100 s^{-1}), it still represents an acceleration of a factor of 10^2 to 10^3 over the spontaneous dissociation rate of GDP from the GTPase in the absence of the exchange factor. A peculiarity of the homologous Vps9p.Ypt51p and Rabex-5.Rab5 systems is that exchange activity at realistic physiological protein concentrations is much weaker for GTP than for GDP, a feature not seen for other systems investigated or for DSS4.Ypt1p, as described here.

It should be noted that all experiments reported here have been performed with Rab proteins that are not post-translationally modified (i.e. C-terminally prenylated). It is possible that there will be some influence of this modification, or in particular of the membrane-bound localisation of the Rab proteins, on the interaction with the proteins showing exchange activity used here. Indeed, in the case of a protein (Rab3 GEPII) identified as an exchange factor for Rab3, it was shown that exchange was dependent on prenylation, or at least that the exchange reaction was enhanced on prenylation.[33] However, the exchange activity of MSS4, the mammalian counterpart of DSS4, on Rab3 was reported in the same contribution to be prenylation-independent. It is presently not technically convenient to produce large quantities of geranylgeranylated Rabs to perform the kind of experiments reported here, but it seems unlikely that the fundamental principles of the interactions will be changed. What seems more likely is that the main effect of membrane localization of Rabs on their interaction with molecules showing exchange activity will be on the affinity between the two proteins, but not on the details of the actual exchange mechanism, so that the rates of exchange determined at saturating concentrations are likely to be valid.

Reasons for the weak exchange activity must be sought at the mechanistic as well as the cell-biological level. Vps9p, and most probably Rabex-5 by homology, together with cdc25 as an exchanger for Ras,[34] have a significantly lower affinity than GDP or GTP for their cognate GTPases, so that they are thermodynamically less able to compete with the nucleotide ligands. The ''fast'' exchangers,

Table 6. Summary of kinetic and thermodynamic constants for the interaction of the Ypt1p, DSS4 and guanosine nucleotides

GDP:			
$K_{1a} = 3.8 \times 10^3$ M^{-1}	$k_{+2} = 1.0 \times 10^6$ M^{-1} s^{-1}	$K_3 = 6 \times 10^4 M^{-1}$	$K_{4a} = 6.6 \times 10^4$ M^{-1}
$k_{+1b} = 39.5$ s^{-1}	$k_{-2} = 7.2 \times 10^{-4}$ s^{-1}		$k_{+4b} = 1.3 \times 10^{-2}$ s^{-1}
$k_{-1b} = 6 \times 10^{-5} s^{-1}$	$K_2 = 1.7 \times 10^9$ M^{-1}		$k_{-4b} = 1.1 \times 10^{-2}$ s^{-1}
$K_1 = 2.5 \times 10^9$ M^{-1}			$K_4 = 1.4 \times 10^5$ M^{-1} s^{-1}
GTP:			
$K_{1a} = 3.3 \times 10^3$ M^{-1}	$k_{+2} = 1.0 \times 10^6$ M^{-1} s^{-1}	$K_3 = 3.1 \times 10^4$ M^{-1}	$K_{4a} = 3.2 \times 10^4$ M^{-1}
$k_{+1b} = 38.6$ s^{-1}	$k_{-2} = 7.2 \times 10^{-4}$ s^{-1}	$k_{-3} = 3.2 \times 10^{-2}$ s^{-1}	$k_{+4b} = 3.2 \times 10^{-2}$ s^{-1}
$k_{-1b} = 5 \times 10^{-5}$ s^{-1}	$K_2 = 1.7 \times 10^9$ M^{-1}	$(k_{+3} = 9.9 \times 10^2 M^{-1}$ $s^{-1})$	$k_{-4b} = 1.6 \times 10^{-2}$ s^{-1}
$K_1 = 3.2 \times 10^9$ M^{-1}			$K_4 = 9.6 \times 10^4$ M^{-1}

The values in parentheses are calculated.

such as RCC1 and EF-Ts, have affinities that are at least as high as those of the nucleotides for the respective GTPases, thus giving them more thermodynamic ''power''. However, DSS4 has an affinity for Ypt1p that is similar to that of GDP, so that the thermodynamic potential for efficient GDP displacement is, in principle, present in the system. The fact that the maximal dissociation rate of GDP from the ternary complex is as slow as in the other two systems suggests that this relative kinetic stability, which leads to a long lifetime of the ternary complexes, is a necessary requirement for its mode of action for all three systems, but particularly in the case of DSS4, where the lifetime of the protein-protein interaction is extended even further by a phenomenon that has not been observed for any of the other exchangers examined in this or in other work. While, in general, the rate constant for the association of nucleotides with the binary complex between GTPase and exchange factor is at least as fast as for the GTPase alone, in the case of the DSS4.Ypt1p complex it is reduced by more than three orders of magnitude in comparison with association with the GTPase alone. Thus, in the normal cycle of activity, after the slow step of GDP dissociation in this system, the binary complex has a relatively long half-life (at saturating GTP concentration several tens of seconds) before dissociation into free DSS4 and Ypt1p.GTP. This is in strong contrast to the situation with Ypt51p and Vps9p or Rab5 and Rabex-5, which after losing GDP are dissociated rapidly by GTP into the GTPase.GTP complex and exchange factor. The question then arises as to whether the long lifetime of the protein-protein complex in the case of Ypt1p and DSS4, which is a thermodynamic consequence of the higher affinity between the two proteins, is of significance for the biological activity of Ypt1p. Since Ypt1p is located in the membrane of the compartments, that it is involved in regulating, this would mean that DSS4 is held in this location for a relatively long period and, since it is clear from other exchange systems that the step of GTP-induced dissociation can in fact be very rapid, it seems likely that this relatively long period of location at the membrane is of functional significance. Our results thus qualify and extend the suggestion made[18,19] that MSS4 and DSS4 are not simply nucleotide-exchange factors but act as ''chaperones'' for the nucleotide-free state of the cognate Rab protein. However, the basis for this is not simply the high affinity of MSS4 or DSS4 for the nucleotide-free GTPase, since this is a fundamental property of all exchange systems examined so far for the Ras superfamily. Our results show that it is the specific property of slow association of GTP with the binary complex of the exchange factor and the GTPase, in contrast to the much faster rate seen in all other systems examined.

The cell-biological significance of the properties reported here could be that the overall cycling time of Rab activity (and therefore of vesicular fusion activity) is strictly controlled by the limited rate of GDP release (or more importantly regeneration of the active GTP complex). In the case of DSS4, it is possible that the long lifetime of its complex with its cognate GTPase allows a further interaction specific for this state to occur.

Materials and Methods

Cloning of Ypt51p, Vps9p, Ypt51p (W61FW101F), DSS4, Ypt1p and Rabex-5

The cDNA of *Saccharomyces cerevisiae* was used in a PCR amplification reaction to produce the coding sequence of Ypt51p,Vps9p and DSS4. The following primers, containing a *Nde*I and *Xho*I restriction site, were used for the cloning of Ypt51p and Vps9p: Vps9p *Nde*I remover, 5′-GGTTAAATCTTTCATGTGCTCATCGTCTAATGG-3′; Vps9 *Nde*I forward, 5′-GAATCAACACATATGACTGATGATGAAAAGAGGG-3′; Vps9 *Xho*I reverse, 5′-TATGTGCTCGAGATCATTATTCTGACAGAGAAAG-3′; Ypt51p *Nde*I forward, 5′-TCACACAAACATATGAACACATCAGTCACTTCC-3′; Ypt51p *Xho*I reverse, 5′-TTTATTCTCGAGTCACTAACAACTGCAAGCACTG-3′.

The forward and reverse primers to amplify the coding sequence of DSS4 had the following sequences and contain a *Bsp*HI or *Sal*I restriction site, respectively: DSS4 *Bsp*HI forward, 5′-GAATAACAGAGATCATGAGCAAGGCTACGTGTTCCTTTG-3′; DSS4 *Sal*I reverse, 5′-GTGCCTGTCGACCTAATTCCTTCCCATAATTTG-3′.

The coding sequence of Vps9p contains an *Nde*I restriction site, which had to be removed for the cloning procedure. Therefore, in a first PCR reaction the Vps9p *Nde*I forward and Vps9p *Xho*I reverse primers were used. The resulting 1353 bp fragment was used as a template in a second PCR reaction using the *Nde*I forward and Vps9p *Nde*I remover primers in order to mutate the *Nde*I sequence CATATG to CACATG without a change in the amino acid sequence. The resulting ca 600 bp fragment was used as a mega primer with the Vps9p *Xho*I reverse primer in a third PCR reaction using the amplification product of the first PCR reaction as a template.

The sequence of Ypt51p and DSS4 was produced in a PCR reaction using the above-mentioned primers. The PCR fragment of DSS4 was restricted with *Bsp*HI and *Sal*I and could be ligated with the pET19b-TEV vector restricted with *Nco*I and *Sal*I. The PCR products of Ypt51p and Vps9p restricted with *Nde*I and *Xho*I were cloned into the pET19b-TEV vector pre-cut with the same enzymes. For construction of the pET19b-TEV expression plasmid, see Alexandrov *et al*.[35] The integrity of the reading frame and the coding sequence was determined by nucleotide sequencing.

Mutations of the tryptophan residues at positions 61 and 101 of Ypt51p were introduced PCR using the following primers: W61F *Bgl*II forward, 5′-AGTTTGAGATCTTCGACACTGCTGGGCAAGAG-3′; W61F *Bgl*II reverse, 5′-TGTCCCAGATCTCAAACTTAACAGTATGTTC-3′; W101F *Sac*I forward, 5′-GTAAAGGAGCTCCATGAACAGGCATCAAAGG-3′; W101F *Sac*I reverse, 5′-TTCATGGAGCTCCTTTACGAAGTGGCGCGCTTTAATAAAGG-3′.

The TGG sequence coding for tryptophan residues was mutated to TTC coding for phenylalanine residues. The primers used contain a *Bgl*II restriction site at position 61 and a *Sac*I restriction site at position 101. In two PCR reactions using the *Bgl*II forward and *Sac*I reverse primer or the *Sac*I forward and the *Bgl*II reverse primer,

two fragments of ca 6200 bp and ca 120 bp were amplified. After restriction with the corresponding enzymes these fragments were ligated. The presence of mutations and the integrity of coding sequence were verified by DNA sequencing.

To generate the pET19b-TEV-Ypt1p vector, the coding sequence excised from the pLN-Ypt1p vector[36] using *Nde*I and *Bam*HI sites was subcloned into the pET19b-TEV expression vector. To generate the pET19b-Rabex-5 vector, the Rabex-5 fragment was restricted from the pQE30 vector[37] and subcloned in the original pET19b vector.

Expression and purification of proteins

Rab5 was expressed and purified as described.[21] Expression and purification of TEV protease was performed as described.[38] To express and purify Vps9p, Ypt51p, Ypt51p(W61FW101F), Ypt1p and DSS4 *Escherichia coli* BL21DE3, cells transformed with the corresponding vectors were grown in Luria-Bertani medium supplemented with 100μg/ml ampicillin at 37 °C and induced at an $A_{600} = 0.7$ with 0.1 mM IPTG. After induction, the cells containing the Ypt51p, Ypt51p(W61FW101F) or Ypt1p plasmids were allowed to grow at 37 °C for an additional three hours. For the expression of Vps9p and DSS4, the temperature was reduced to 20 °C and the cells were harvested after five hours of induction. The expressed proteins have an N-terminal 6 × His affinity tag that can be removed by TEV protease.

After harvesting the cells by centrifugation, they were resuspended in lysis buffer containing 50 mM sodium phosphate (pH 8.0), 300 mM sodium chloride and 5 mM β-mercaptoethanol (for purification of the GTPases, 5 mM magnesium chloride and 5μM GDP were additionally added in all buffers used in the purification procedure) and lysed using a fluidizer (Microfluidics Corperation). The lysate was clarified by ultracentrifugation for one hour at 4 °C. The 6 × His-tagged proteins were purified using Ni-NTA-superflow matrix (Qiagen) according to the manifacturer's guidelines. Eluates were analyzed by SDS-PAGE followed by Coomassie blue staining. Fractions containing the proteins were pooled. After ammonium sulphate precipitation (final 70 % (w/v)) the protein pellet was resuspended in 25 mM sodium phosphate buffer (pH 8.0), 5 mM β-mercaptoethanol. TEV protease (itself containing a 10 × His N-terminal affinity tag) was added and the reaction mixture was incubated at room temperature. After TEV-cleavage, the protein solution was passed over a second Ni-NTA column pre-equilibrated with 25 mM sodium phosphate buffer (pH 7.5), 50 mM sodium chloride, 5 mM β-mercaptoethanol in order to remove the polyhistidine tags, uncleaved protein and the TEV protease. After concentrating the fractions containing the cleaved protein, the solution was loaded onto a Superdex 75 16/60 gel-filtration column (Pharmacia) pre-equilibrated with a buffer consisting of 40 mM Hepes buffer (pH 7.5), 100 mM sodium chloride and 5 mM β-mercaptoethanol. Fractions were analyzed by SDS-PAGE and fractions containing pure protein were pooled, concentrated and stored in multiple aliquots at −80 °C. Typical purity was over 98 % as judged by Coomassie blue staining and ESI-MS.

For Rabex-5, the principal expression and purification protocol was according to that described above but the instability and the low expression level of soluble protein precluded TEV cleavage, and Rabex-5 was used as a His-tagged protein. For the production of soluble Rabex-5, the temperature was reduced to 20 °C after induction and cells were grown for an additional two hours. The lysis buffer contained 50 mM sodium phosphate (pH 8.0), 500 mM sodium chloride, 5 mM β-mercaptoethanol and a mixture of the protease inhibitors PMFS, aprotinin, leupeptin, chymostatin and pepstatin. The His-tagged protein was purified using Ni-NTA-superflow matrix (Qiagen) according to the manufacturer's guidelines. Eluates were analysed by SDS-PAGE followed by Coomassie blue staining. Fractions containing the protein were pooled and dialysed against 25 mM Hepes (pH 7.5), 500 mM NaCl, 5 mM β-mercaptoethanol. Further purification was performed on a Superdex 75 16/60 gel-filtration column (Pharmacia) pre-equilibrated with the same buffer. The purified protein was used directly for the kinetic experiments, because freezing and storing at −80 °C caused inactivation.

Nucleotide exchange

The tightly bound GDP present in the purified Ypt51p, Rab5 and Ypt1p was exchanged against other nucleotides (mantGDP, mantGppNHp or GppNHp) in the presence of EDTA, followed by gel-filtration to remove excess nucleotide.

Preparation of nucleotide-free GTPases

Nucleotide-free Rab5, Ypt51p and Ypt1p were prepared as described.[21,22]

Labelling of proteins with 5-({[(2-iodoacetyl)amino]ethyl}amino)naphthalene-1sulphonic acid (1,5-IAEDANS)

Cysteine residues were labelled as described.[35] The labelling was analysed by SDS-PAGE and ESI-MS.

Fluorescence measurements

All fluorescence measurements were carried out in a buffer containing 40 mM Hepes (pH 7.5), 5 mM $MgCl_2$ and 5 mM β-mercaptoethanol at 25 °C. Fluorescence spectra and long-time fluorescence measurements were performed with an SLM 8100 spectrophotometer (Amicon, Silver Spring, MD, USA) or with a Fluoroscan Ascent FL 1.8 (Labsystems). Tryptophan fluorescence was excited at 290 nm and detected at 340 nm. Fluorescence of mant nucleotides was excited directly at 356 nm or *via* fluorescence resonance energy transfer (FRET) at 290 nm and detected at 440 nm. For measurement of the dansyl fluorescence signal, the dansyl group was excited directly at 364 nm or *via* FRET at 290 nm and data were collected at 480 nm.

Rapid kinetics were examined with a stopped flow apparatus (High Tech Scientific, Salisbury, United Kingdom). Excitation of tryptophan fluorescence was at 296 nm, with detection through a 320 nm cut-off filter. Fluorescence of mant nucleotides was excited either directly at 290 nm or *via* FRET at 365 nm, with emission through a 389 nm cut-off filter. The dansyl fluorescence was excited *via* FRET at 296 nm and detected through a 389 nm cut-off filter. Data collection and primary analysis for determination of rate constants were performed with the package from High Tech Scientific, while sec-

ondary analysis was done with the program Graphit 3.0 (Erithacus software).

Acknowledgements

We thank Heino Prinz for mass spectrometry, Andrea Beste for synthesis of the nucleotides, D. Gallwitz for the pLN-Ypt1p vector and E. Rostkova for the purification of Ypt1p and DSS4. We gratefully acknowledge support by a post-doctoral fellowship from EMBO (N.T.) and grants to K.A. (Al 484/1-1) and A.J.S. (Sch 545/1-2) from the Deutsche Forschungsgemeinschaft.

References

1. Zerial, M. & Stenmark, H. (1993). Rab GTPases in vesicular transport. *Curr. Opin. Cell Biol.* **5**, 613-620.
2. Novick, P. & Brennwald, P. (1993). Friends and family: the role of the Rab GTPases in vesicular traffic. *Cell,* **75**, 597-601.
3. Pfeffer, S. R. (1994). Rab GTPases: master regulators of membrane trafficking. *Curr. Opin. Cell Biol.* **6**, 522-526.
4. Novick, P. & Zerial, M. (1997). The diversity of Rab proteins in vesicle transport. *Curr. Opin. Cell Biol.* **9**, 496-504.
5. Martinez, O. & Goud, B. (1998). Rab proteins. *Biochim. Biophys. Acta,* **1404**, 101-112.
6. Chavrier, P. & Goud, B. (1999). The role of ARF and Rab GTPases in membrane transport. *Curr. Opin. Cell Biol.* **11**, 466-475.
7. Schimmoller, F., Simon, I. & Pfeffer, S. R. (1998). Rab GTPases, directors of vesicle docking. *J. Biol. Chem.* **273**, 22161-22164.
8. Albert, S., Will, E. & Gallwitz, D. (1999). Identification of the catalytic domains and their functionally critical arginine residues of two yeast GTPase-activating proteins specific for Ypt/Rab transport GTPases. *EMBO J.* **18**, 5216-5225.
9. Albert, S. & Gallwitz, D. (1999). Two new members of a family of Ypt/Rab GTPase activating proteins. Promiscuity of substrate recognition. *J. Biol. Chem.* **274**, 33186-33189.
10. Walch-Solimena, C., Collins, R. N. & Novick, P. J. (1997). Sec2p mediates nucleotide exchange on Sec4p and is involved in polarized delivery of post-Golgi vesicles. *J. Cell Biol.* **137**, 1495-1509.
11. Hama, H., Tall, G. G. & Horazdovsky, B. F. (1999). Vps9p is a guanine nucleotide exchange factor involved in vesicle- mediated vacuolar protein transport. *J. Biol. Chem.* **274**, 15284-15291.
12. Horiuchi, H., Lippe, R., McBride, H. M., Rubino, M., Woodman, P. & Stenmark, H. *et al*. (1997). A novel Rab5 GDP/GTP exchange factor complexed to Rabaptin-5 links nucleotide exchange to effector recruitment and function. *Cell,* **90**, 1149-1159.
13. Burstein, E. S. & Macara, I. G. (1992). Characterization of a guanine nucleotide-releasing factor and a GTPase-activating protein that are specific for the ras-related protein p25rab3A. *Proc. Natl Acad. Sci. USA,* **89**, 1154-1158.
14. Burton, J., Roberts, D., Montaldi, M., Novick, P. & De Camilli, P. (1993). A mammalian guanine-nucleotide-releasing protein enhances function of yeast secretory protein Sec4. *Nature,* **361**, 464-467.
15. Burton, J. L., Burns, M. E., Gatti, E., Augustine, G. J. & De Camilli, P. (1994). Specific interactions of Mss4 with members of the Rab GTPase subfamily. *EMBO J.* **13**, 5547-5558.
16. Moya, M., Roberts, D. & Novick, P. (1993). *DSS4-1* is a dominant suppressor of *sec4-8* that encodes a nucleotide exchange protein that aids Sec4p function. *Nature,* **361**, 460-463.
17. Burton, J. L., Slepnev, V. & De Camilli, P. V. (1997). An evolutionarily conserved domain in a subfamily of Rabs is crucial for the interaction with the guanyl nucleotide exchange factor Mss4. *J. Biol. Chem.* **272**, 3663-3668.
18. Nuoffer, C., Wu, S. K., Dascher, C. & Balch, W. E. (1997). Mss4 does not function as an exchange factor for Rab in endoplasmic reticulum to Golgi transport. *Mol. Biol. Cell,* **8**, 1305-1316.
19. Collins, R. N., Brennwald, P., Garrett, M., Lauring, A. & Novick, P. (1997). Interactions of nucleotide release factor Dss4p with Sec4p in the post-Golgi secretory pathway of yeast. *J. Biol. Chem.* **272**, 18281-18289.
20. Burd, C. G., Mustol, P. A., Schu, P. V. & Emr, S. D. (1996). A yeast protein related to a mammalian Ras-binding protein, Vps9p, is required for localization of vacuolar proteins. *Mol. Cell Biol.* **16**, 2369-2377.
21. Simon, I., Zerial, M. & Goody, R. S. (1996). Kinetics of interaction of Rab5 and Rab7 with nucleotides and magnesium ions. *J. Biol. Chem.* **271**, 20470-20478.
22. John, J., Sohmen, R., Feuerstein, J., Linke, R., Wittinghofer, A. & Goody, R. S. (1990). Kinetics of interaction of nucleotides with nucleotide-free H-ras p21. *Biochemistry,* **29**, 6058-6065.
23. Moser, C., Mol, O., Goody, R. S. & Sinning, I. (1997). The signal recognition particle receptor of *Escherichia coli* (FtsY) has a nucleotide exchange factor built into the GTPase domain. *Proc. Natl Acad. Sci. USA,* **94**, 11339-11344.
24. Esters, H., Alexandrov, K., Constantinescu, A. T., Goody, R. S. & Scheidig, A. J. (2000). High-resolution crystal structure of *S. cerevisiae* Ypt51(DeltaC15)-GppNHp, a small GTP-binding protein involved in regulation of endocytosis. *J. Mol. Biol.* **298**, 111-121.
25. Wagner, A., Simon, I., Sprinzl, M. & Goody, R. S. (1995). Interaction of guanosine nucleotides and their analogs with elongation factor Tu from *Thermus thermophilus*. *Biochemistry,* **34**, 12535-12542.
26. Klebe, C., Prinz, H., Wittinghofer, A. & Goody, R. S. (1995). The kinetic mechanism of Ran – nucleotide exchange catalyzed by RCC1. *Biochemistry,* **34**, 12543-12552.
27. Melchior, F., Paschal, B., Evans, J. & Gerace, L. (1993). Inhibition of nuclear protein import by non-hydrolyzable analogues of GTP and identification of the small GTPase Ran/TC4 as an essential transport factor (published erratum appears in *J. Cell Biol.* (1994) **124**, 217). *J. Cell Biol.* **123**, 1649-1659.
28. Moore, M. S. & Blobel, G. (1993). The GTP-binding protein Ran/TC4 is required for protein import into the nucleus. *Nature,* **365**, 661-663.
29. Klebe, C., Nishimoto, T. & Wittinghofer, F. (1993). Functional expression in *Escherichia coli* of the mitotic regulator proteins p24ran and p45rcc1 and fluorescence measurements of their interaction. *Biochemistry,* **32**, 11923-11928.
30. Klebe, C., Bischoff, F. R., Ponstingl, H. & Wittinghofer, A. (1995). Interaction of the nuclear

GTP-binding protein Ran with its regulatory proteins RCC1 and RanGAP1. *Biochemistry,* **34**, 639-647.
31. Klebe, C., Prinz, H., Wittinghofer, A. & Goody, R. S. (1995). The kinetic mechanism of Ran - nucleotide exchange catalyzed by RCC1. *Biochemistry*, **34**, 12543-12552.
32. Hwang, Y. W. & Miller, D. L. (1985). A study of the kinetic mechanism of elongation factor Ts. *J. Biol. Chem.* **260**, 11498-11502.
33. Wada, M., Nakanishi, H., Satoh, A., Hirano, H., Obaishi, H., Matsuura, Y. & Takai, Y. (1997). Isolation and characterization of a GDP/GTP exchange protein specific for the Rab3 subfamily small G proteins. *J. Biol. Chem.* **272**, 3875-3878.
34. Lenzen, C., Cool, R. H., Prinz, H., Kuhlmann, J. & Wittinghofer, A. (1998). Kinetic analysis by fluorescence of the interaction between Ras and the catalytic domain of the guanine nucleotide exchange factor Cdc25Mm. *Biochemistry,* **37**, 7420-7430.
35. Alexandrov, K., Simon, I., Yurchenko, V., Iakovenko, A., Rostkova, E., Scheidig, A. J. & Goody, R. S. (1999). Characterization of the ternary complex between Rab7, REP-1 and Rab geranylgeranyl transferase. *Eur. J. Biochem.* **265**, 160-170.
36. Wagner, P., Hengst, L. & Gallwitz, D. (1992). Ypt proteins in yeast. *Methods Enzymol.* **219**, 369-387.
37. Rybin, V., Ullrich, O., Rubino, M., Alexandrov, K., Simon, I. & Seabra, M. C. *et al*. (1996). GTPase activity of Rab5 acts as a timer for endocytic membrane fusion. *Nature,* **383**, 266-269.
38. Parks, T. D., Leuther, K. K., Howard, E. D., Johnston, S. A. & Dougherty, W. G. (1994). Release of proteins and peptides from fusion proteins using a recombinant plant virus proteinase. *Anal. Biochem.* **216**, 413-417.

Edited by J. Karn

(Received 2 January 2001; received in revised form 3 May 2001; accepted 3 May 2001)